Plasma Science and Technology

PAPER

The investigation of OH radicals produced in a DC glow discharge by laser-induced fluorescence spectrometry

To cite this article: Feng LIU *et al* 2021 *Plasma Sci. Technol.* **23** 064002

View the article online for updates and enhancements.

This content was downloaded from IP address 210.73.19.177 on 15/03/2021 at 01:54

© 2021 Hefei Institutes of Physical Science, Chinese Academy of Sciences and IOP Publishing Printed in China and the UK

Plasma Sci. Technol. **23** (2021) 064002 (9pp) https://doi.org/10.1088/2058-6272/abe3e1

The investigation of OH radicals produced in a DC glow discharge by laser-induced fluorescence spectrometry

Feng LIU (刘峰)[1], **Yue ZHUANG** (庄越)[1], **Haijing CHU** (储海靖)[1], **Zhi FANG** (方志)[1] **and Wenchun WANG** (王文春)[2,3]

[1] College of Electrical Engineering and Control Science, Nanjing Tech University, Nanjing 211816, People's Republic of China
[2] Key Lab of Materials Modification, Dalian University of Technology, Ministry of Education, Dalian 116024, People's Republic of China
[3] School of Physics and Optoelectronic Technology, Dalian University of Technology, Dalian 116024, People's Republic of China

E-mail: fangzhi@njtech.edu.cn

Received 25 November 2020, revised 30 January 2021
Accepted for publication 5 February 2021
Published 11 March 2021

Abstract

In this paper the OH radicals produced by a needle–plate negative DC discharge in water vapor, $N_2 + H_2O$ mixture gas and $He + H_2O$ mixture gas are investigated by a laser-induced fluorescence (LIF) system. With a ballast resistor in the circuit, the discharge current is limited and the discharges remain in glow. The OH rotation temperature is obtained from fluorescence rotational branch fitting, and is about 350 K in pure water vapor. The effects of the discharge current and gas pressure on the production and quenching processes of OH radicals are investigated. The results show that in water vapor and $He + H_2O$ mixture gas the fluorescence intensity of OH stays nearly constant with increasing discharge current, and in $N_2 + H_2O$ mixture gas the fluorescence intensity of OH increases with increasing discharge current. In water vapor and $N_2 + H_2O$ mixture gas the fluorescence intensity of OH decreases with increasing gas pressure in the studied pressure range, and in $He + H_2O$ mixture gas the fluorescence intensity of OH shows a maximum value within the studied gas pressure range. The physicochemical reactions between electrons, radicals, ground and metastable molecules are discussed. The results in this work contribute to the optimization of plasma reactivity and the establishment of a molecule reaction dynamics model.

Keywords: laser-induced fluorescence, OH radicals, rotational temperature, water vapor

(Some figures may appear in colour only in the online journal)

1. Introduction

Non-thermal plasmas, characterized by a low gas temperature and high electron temperature, are energy efficient because most electrical energy goes into the generation of energetic electrons rather than gas heating. Such plasmas are widely used in fields ranging from material surface modification [1, 2] and environmental pollution control [3, 4] to plasma medicine [5, 6]. The reactive species in a non-thermal plasma play an important role in the material, chemical and biological applications by participating in physicochemical reactions [7, 8]. In plasmas generated in air, the most common reactive species are reactive oxygen species (ROS) and reactive nitrogen species [7]. ROS, including O, O_3, H_2O_2 and OH, exhibit a strong oxidation ability and are key participants in applications including SO_2/NO_x removal, decomposition of volatile organic compounds, medical sterilization and hydrophilic modification of material surfaces [9–12]. Among the ROS, OH radicals, which have the strongest oxidation ability, play a key role in the physicochemical processes of

those applications. Therefore, researchers have investigated OH radicals in various plasmas, such as glow discharges [13, 14], corona discharges [15, 16] and arc discharges [17, 18], to improve the treatment effects.

To further enhance the practical applications of non-thermal plasmas, it is necessary to diagnose and monitor the kind and amount of reactive species in discharges, especially OH radicals. Many researchers have devoted much effort to measuring the optical emission spectra (OES), laser-induced fluorescence (LIF) spectra, density and lifetime of OH radicals to enhance the number of OH radicals in different kinds of discharges and various electrical structures [19–22]. Liu *et al* measured the OES intensity and spatial distribution of OH radicals in a $N_2 + H_2O$ mixture gas needle–plate and wire–plate pulsed corona streamer discharge and optimized the emission intensity of OH radicals by adjusting the voltage, frequency and O_2 addition [10, 23–25]. The production and depletion of OH, O, and H were also calculated from the recorded emission intensities, reaction processes and corresponding reaction rates [26]. Dilecce *et al* [21, 27] studied OH radicals in He/H_2O and Ar/H_2O pulsed dielectric barrier discharges, and pointed out that water vapor content and gas composition might change the microscopic process of plasma chemistry, which in turn changes the spatial and temporal distribution of OH radicals. Sainct *et al* [28] reported the lifetime of OH radicals produced in a nanosecond pulsed water vapor discharge to be about 50 μs. Ono *et al* [29, 30] investigated the decay behavior of OH radicals in a pulsed pin–plate corona discharge and measured the spatial and temporal distribution of OH density in a He/H_2O atmospheric pressure jet by LIF and found that OH radicals were primarily produced by the recombination of H_2O^+ rather than electron-impact dissociation of H_2O.

Although there are already some findings regarding the detection and the applications of OH radicals, the production and quenching processes of OH radicals are still not clear due to their short lifetime and strong reactivity with surrounding particles. In different gas systems, the kinetics of the chemical reaction-related OH production and quenching are complex. Without a further understanding of the production and quenching processes of OH radicals it is difficult to optimize the number of OH radicals by simply adjusting the process parameters. For the purpose of enhancing plasma reactivity and optimizing the effects of plasma treatments it is important to reveal the kinetics of the chemical reaction-related OH radicals.

In this paper, the OH radicals produced by a needle–plate negative DC discharge in water vapor, $N_2 + H_2O$ mixture gas and $He + H_2O$ mixture gas are investigated with a LIF system. The rotational temperature of OH radicals is calculated by fitting the fluorescence rotational branches. By adjusting the discharge current using the applied voltage and gas pressure, the main physicochemical reaction is discussed and the effects of the collision frequency between particles on the production and quenching processes of OH radicals are investigated. The findings in this work will help enhance plasma reactivity and the plasma treatment effect.

2. Experimental setup

The experimental setup is shown in figure 1(a). It comprises a high-voltage negative DC power supply, a discharge reactor, a gas system and a LIF system. The high-voltage negative DC power supply can provide a stable high-voltage negative DC of 0 to −60 kV. A ballast resistor of 3 MΩ is used to prevent glow to arc transition. The discharge reactor is made of stainless steel and can be pumped to vacuum to control the gas component inside the reactor. The needle–plate electrodes are placed in the center of the reactor to generate plasma between the electrodes. The needle electrode is made of tungsten with a diameter of 0.8 mm. The plate electrode is made of stainless steel with a diameter of 30 mm. The gap between the needle–plate electrodes can be adjusted from 0 to 50 mm, and is fixed at 8 mm during the experiment. The voltage is recorded by a high-voltage probe (Tektronix, P6015A) and an oscilloscope (Tektronix, TDS3052B). The current is measured by a current meter. The discharge images are recorded by a digital camera (Canon EOS 6D). High-purity gases He (99.999%) and N_2 (99.999%) are used. The supply gas bubbles the water to control humidity at 10% in the $N_2 + H_2O$ mixture gas and $He + H_2O$ mixture gas.

The LIF system consists of a laser system with a Nd:YAG laser (Quanta-Ray GCR-170, fixed frequency 10 Hz) and a tunable dye laser (Lumonics HD-500) and a detection system with a photomultiplier tube (PMT; Hamamatsu R699), a convex lens and a band-pass filter with a 308 nm center wavelength, 10 nm bandwidth and maximum transmittance of 20%. The Nd:YAG laser produces a 1064 nm output, which is frequency doubled to 532 nm. The tunable dye laser is pumped by the 532 nm beam from the Nd:YAG laser and produces a 616 nm output, which is frequency doubled by an HT-100 frequency doubling device to 308 nm as the detection laser for ground state OH radicals. The detection laser with an energy of 0.1 mJ/pulse is a 3 mm × 2 mm laser beam passing through the discharge space near the ground electrode as shown in figure 1(b). During the experiment, the fluorescence signal increases linearly with the detection laser energy, indicating no saturation effect in OH radical detection. The fluorescence signal is collected by the PMT and averaged by a boxcar (SRS, SR250). The output analog signal is converted to a digital signal by a digital-to-analog converter and transferred to a computer. The gate width of the boxcar is set at 30 ns and the sampling gate is set at 170 ns after the detection laser, which can avoid interference from the background scattering of the detection laser from the fluorescence signal.

3. Experimental results and discussion

3.1. DC glow discharge plasma

Figures 2(a) and (b), respectively, show the discharge images in air at atmospheric pressure and low pressure (180 Pa) excited by a negative DC voltage. For the discharge at atmospheric pressure in figure 2(a) it can be seen that the discharge image with an exposure time of 1/30 s consists of a

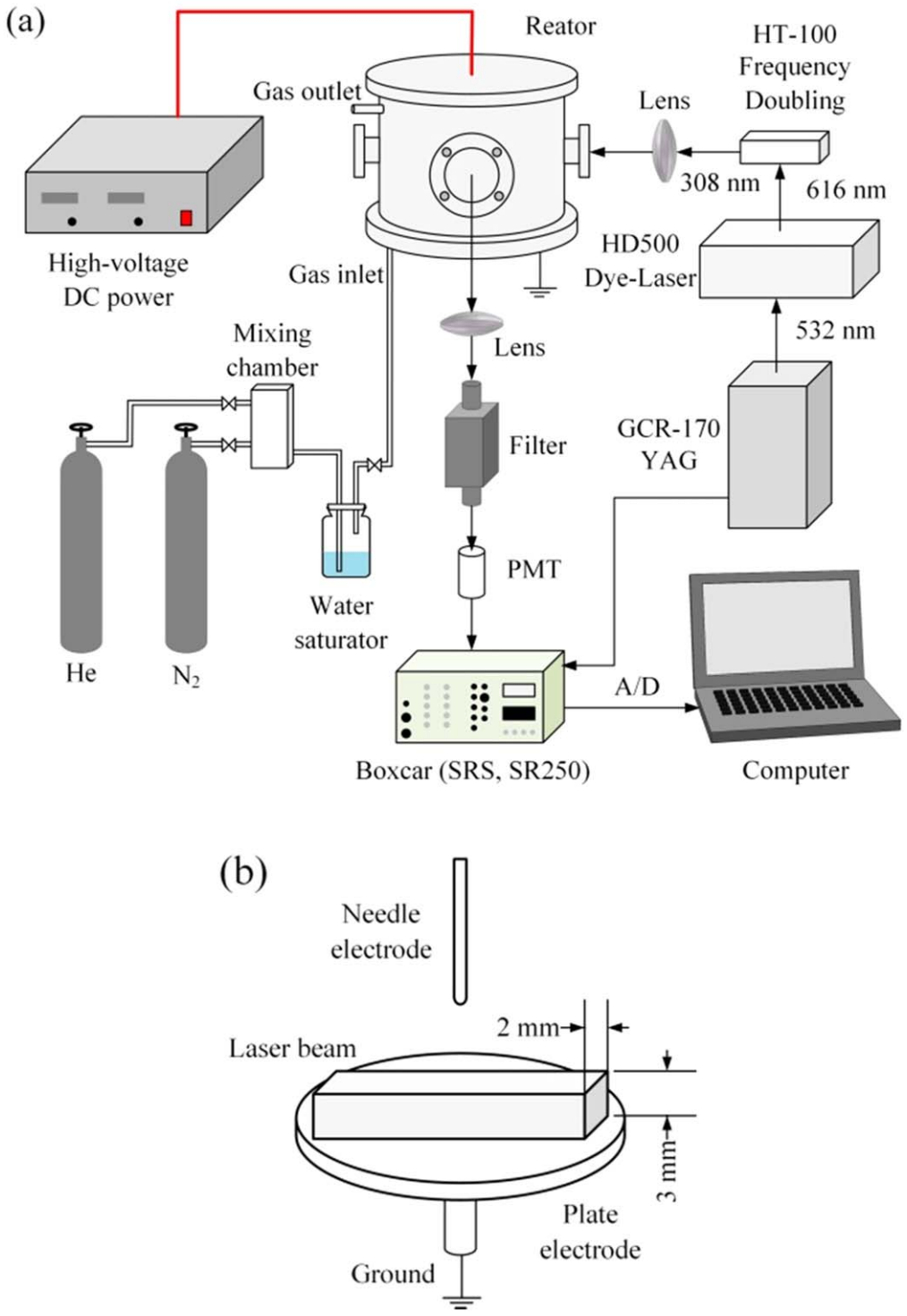

Figure 1. Schematic diagram of the experimental setup (a) and schematic diagram of the detecting laser (b).

negative glow, a Faraday dark space, a positive column and a distinct anode glow from the needle to the plate. With the 10.6 kV applied voltage from the power supply and a 3 MΩ ballast resistor, the voltage between the two electrodes (discharge voltage) is about 1.8 kV, which is far below the ignition voltage for a corona discharge (about 6.5 kV in our experiment), and the recorded discharge current is a steady 2.94 mA, which is different from the pulse behavior of corona and filament modes [31, 32]. At low pressure, the discharge is more diffuse, as shown in figure 2(b), and a longer exposure time 1/8 s is used to enhance the image brightness. The current is 3.11 mA and the discharge voltage is about 450 V. In a glow discharge, the discharge voltage remains almost constant. With a ballast resistor, the regulation of the applied voltage from the power supply results in the variation of the discharge current.

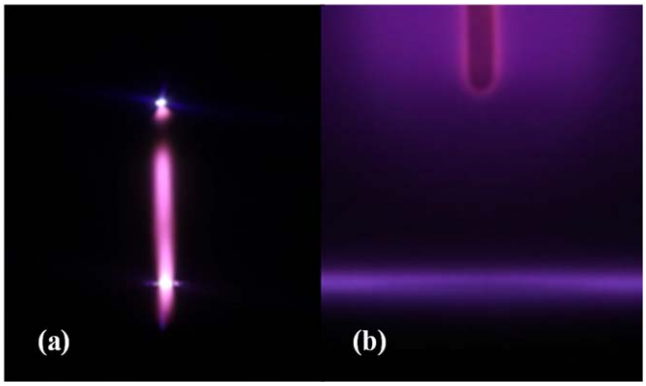

Figure 2. Discharge images of a DC glow discharge at atmospheric pressure (a) and at low pressure (180 Pa) (b).

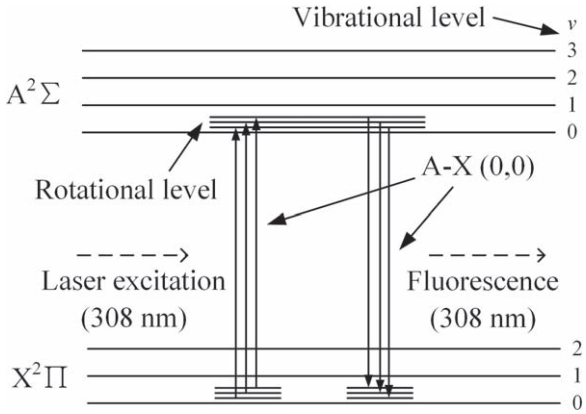

Figure 3. Diagram of the laser-induced fluorescence process in detection of OH ground state radicals.

From the discharge images it can be seen that the plasma has a 'form' and the distribution of active species is related to this form. From the cathode, electrons are emitted from the metal surface. With a high electric field, avalanches of electrons occur and the region of negative glow is characterized by high concentrations of electrons and ions formed. In the negative glow there is a large amount of recombination of ions and electrons. With the energy reduced by ionization collisions, a Faraday dark space is formed with many electrons drifting to the anode. With this gained energy, the positive column is reduced and ionizations of neutral particles occur again. To avoid interference from the recombination of ions and electrons, the detection area for OH radicals is setting near the plate including the anode glow and positive column region with a 3 mm $\times$ 2 mm laser.

3.2. The LIF spectra of OH radicals

In a non-equilibrium plasma excited by high voltage, electrons have a much higher migration rate than ions and can obtain a high energy (1–20 eV) for a long free path in space. Those energetic electrons can efficiently ionize, excite and dissociate background molecules or atoms into active radicals and species [26, 33, 34]. Detection of these excited species can be realized by observing the optical emission spectra but it is hard to detect radicals in the ground state. The LIF diagnosis method gives an opportunity to reveal the information about the ground state radicals without disturbing the discharge processes [35–37]. In this work, we detect the ground state of OH ($X^2\Pi$) by exciting it to the excited state OH ($A^2\Sigma$) with a 308 nm laser and observing the fluorescence of OH ($A^2\Sigma \rightarrow X^2\Pi$ 0–0) with a delay observation window to avoid interference from the input laser. The process is illustrated schematically in figure 3. Under high pressure, the signal-to-noise ratio of LIF measurement is low and it is hard to distinguish the fluorescence spectra. Therefore, the LIF measurement of OH radicals is conducted at low pressure.

To produce a DC glow discharge and detect OH radicals in space, the reactor is filled with water vapor to 230 Pa and the applied voltage is set at -9.5 kV; the current is 2.96 mA. Figure 4 shows the LIF spectrum of OH ($A^2\Sigma \rightarrow X^2\Pi$ 0–0), which contains the Q, R and P rotational branches. The simulated LIF spectrum of OH ($A^2\Sigma \rightarrow X^2\Pi$ 0–0) at 350 K rotational temperature and 230 Pa gas pressure by LIFBASE software is also shown in figure 4 as a comparison. It can be seen that the measured LIF spectrum is very close to the simulated spectrum. Considering the instability of the discharge and the laser source, the rotational temperature of the OH generated in the discharge space is about 350 $\pm$ 30 K.

Ground state OH radicals were also produced in DC discharges in other gas systems to compare the production and quenching processes of OH radicals. Figure 5 shows the LIF spectrum of the OH ($A^2\Sigma \rightarrow X^2\Pi$ 0–0) generated by a negative DC glow discharge in $N_2 + H_2O$ mixture gas with a pressure of 50 Pa and an applied voltage set at -4 kV; the current was 1.21 mA. Figure 6 shows the LIF spectrum of OH ($A^2\Sigma \rightarrow X^2\Pi$ 0–0) generated by a negative DC glow discharge in $He + H_2O$ mixture gas with a pressure of 400 Pa and an applied voltage set at -8 kV; the current was 2.43 mA. It can be seen from figures 5 and 6 that the background noises of the LIF spectra in the $N_2 + H_2O$ and $He + H_2O$ mixture gases are much greater than in pure water vapor (figure 4). This is due to the discharge instability caused by the addition of nitrogen and helium. However, each rotational branch of the LIF spectra of OH ($A^2\Sigma \rightarrow X^2\Pi$ 0–0) can be clearly separated, which can be used for further investigation in the following sections.

3.3. The fluorescence intensity of OH radicals in water vapor

From the observed LIF spectra of OH ($A^2\Sigma \rightarrow X^2\Pi$ 0–0), the fluorescence intensity of the Q1(1) branch is stronger than the other branches and less disturbed by the other fluorescence lines. Therefore, variations of the fluorescence intensity of the Q1(1) branch with different parameters are used to reflect the change in fluorescence intensity of OH ($A^2\Sigma \rightarrow X^2\Pi$ 0–0). Because the applied voltage is the sum of the discharge voltage between the electrodes and the voltage across the ballast resistor, the discharge current is more important for reflecting the plasma conditions. Then, the relation of the discharge current by changing the applied voltage from -5.5 to -10.5 kV and the intensity of the Q1(1) branch at 230 Pa in a pure water vapor system was investigated. The results are shown in figure 7. It

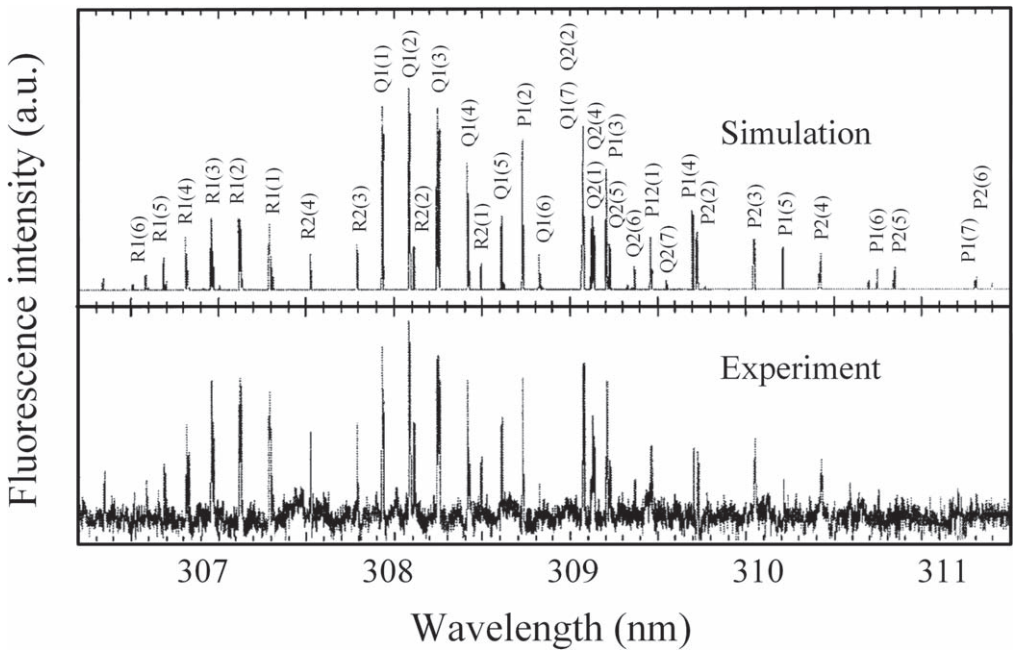

Figure 4. The LIF spectrum of OH ($A^2\Sigma \rightarrow X^2\Pi$ 0–0) in water vapor and the simulation spectrum.

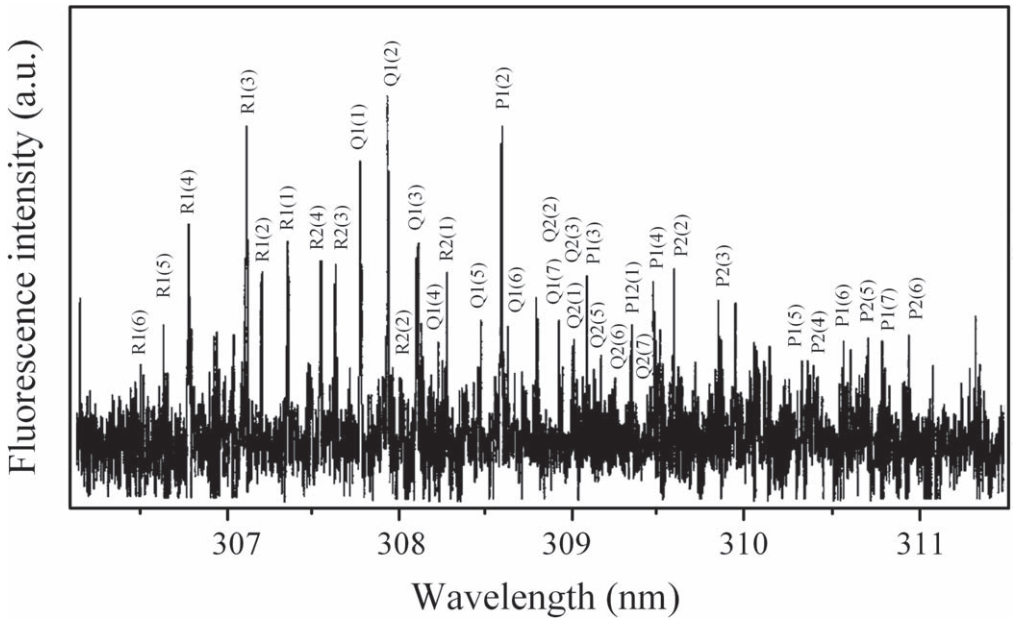

Figure 5. LIF spectrum of OH ($A^2\Sigma \rightarrow X^2\Pi$ 0–0) in $N_2 + H_2O$ mixture gas.

can be seen that the fluorescence intensity of the Q1(1) branch stays nearly constant with increasing discharge current. Figure 8 shows the change in fluorescence intensity of the Q1(1) branch with the variation in pressure at a voltage of −7 kV. It can be seen from figure 8 that the fluorescence intensity of the Q1(1) branch decreases significantly with increasing pressure in the investigated pressure range.

The main physicochemical reactions that produce OH radicals in a water vapor system are as follows [26]:

$$e + H_2O \rightarrow e + H + OH \quad 2.6 \times 10^{-12}\ cm^3\ s^{-1} \quad (1)$$

$$e + H_2O \rightarrow H + OH \quad 2.6 \times 10^{-12}\ cm^3\ s^{-1} \quad (2)$$

$$e + H_2O \rightarrow 2e + H^+ + OH \quad 4.4 \times 10^{-16}\ cm^3\ s^{-1} \quad (3)$$

$$e + H_2O^+ \rightarrow H + OH \quad 3.8 \times 10^{-7}\ cm^3\ s^{-1} \quad (4)$$

$$O(^1D) + H_2O \rightarrow 2OH \quad 2.3 \times 10^{-10}\ cm^3\ s^{-1} \quad (5)$$

where H_2O^+ and $O(^1D)$ are generated by collision of high-energy electrons with water molecules. In the above reactions, the concentrations of H_2O^+ and $O(^1D)$ are very low, the electron energy required for reaction (3) is very high and the reaction rate is very low. Therefore, OH radicals are not mainly produced by reactions (3)–(5), but are produced by the

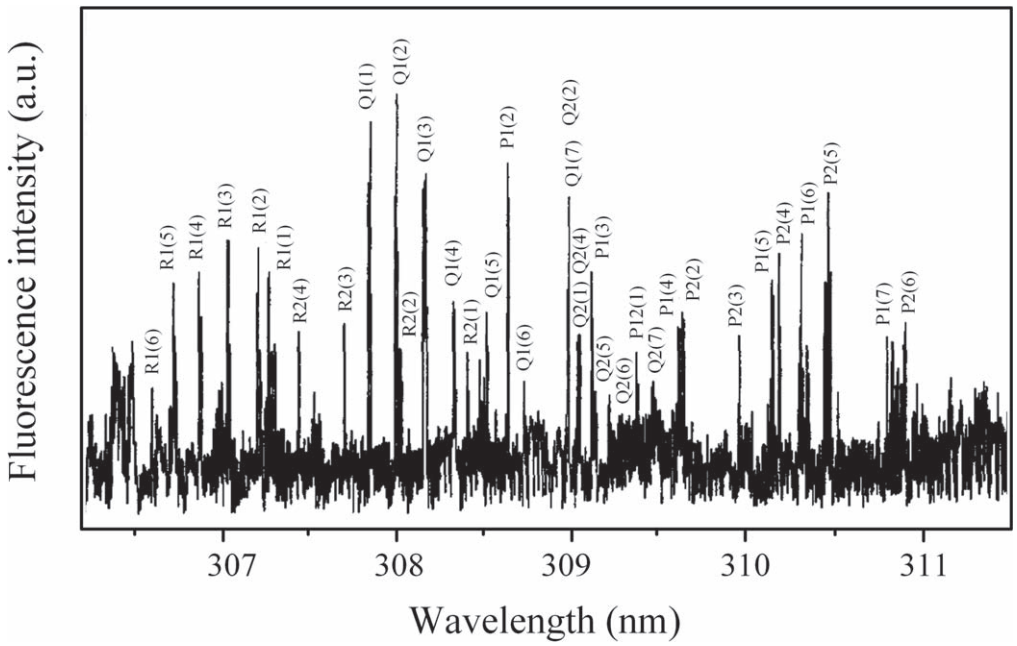

Figure 6. LIF spectrum of OH ($A^2\Sigma \rightarrow X^2\Pi$ 0–0) in He + H_2O mixture gas.

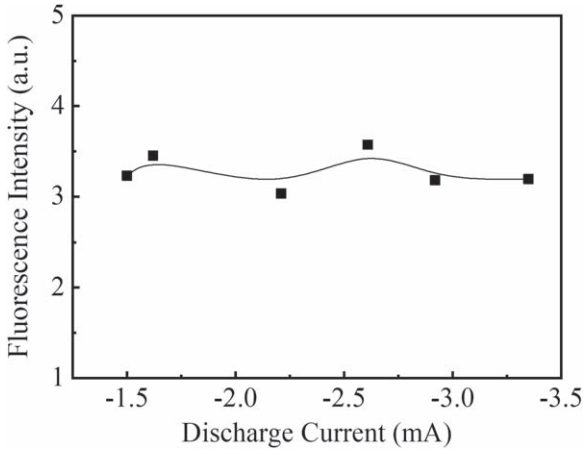

Figure 7. Fluorescence intensity of the Q1(1) branch at different discharge currents in water vapor.

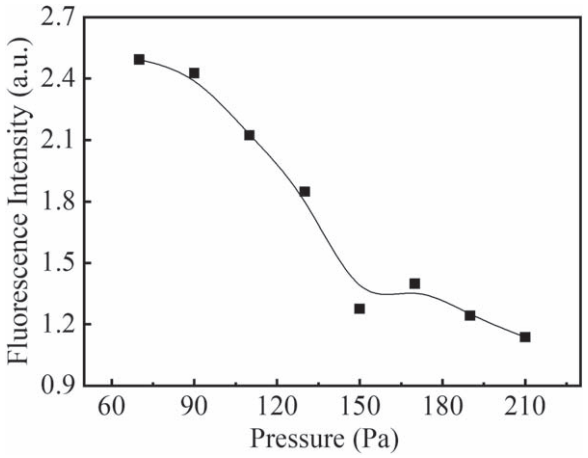

Figure 8. Fluorescence intensity of the Q1(1) branch at different pressures in water vapor.

reactions (1) and (2) by electron and water molecule collision–dissociation reactions.

The main quenching processes of OH radicals in water vapor system are as follows [26]:

$$OH + O \rightarrow H + O_2 \quad 3.8 \times 10^{-11}\,cm^3\,s^{-1} \tag{6}$$

$$OH + O_3 \rightarrow HO_2 + O_2 \quad 6.5 \times 10^{-14}\,cm^3\,s^{-1} \tag{7}$$

$$OH + H_2 \rightarrow H_2O + H \quad 6.7 \times 10^{-15}\,cm^3\,s^{-1} \tag{8}$$

$$OH + HO_2 \rightarrow H_2O + O_2 \quad 1.1 \times 10^{-10}\,cm^3\,s^{-1} \tag{9}$$

$$OH + O^+ \rightarrow OH^+ + O \quad 3.6 \times 10^{-10}\,cm^3\,s^{-1} \tag{10}$$

$$OH + O^+ \rightarrow O_2^+ + H \quad 3.6 \times 10^{-10}\,cm^3\,s^{-1} \tag{11}$$

$$OH + OH \rightarrow H_2O + O \quad 6.6 \times 10^{-33}\exp(-2173/T)\,cm^3\,s^{-1} \tag{12}$$

$$OH + H \rightarrow H_2 + O \quad 1.38 \times 10^{-14}T\exp(-3500/T)\,cm^3\,s^{-1} \tag{13}$$

$$OH + H + M \rightarrow H_2O + M \quad 1.1 \times 10^{-23}T^{-2.6}\,cm^6\,s^{-1} \tag{14}$$

where T is the gas temperature. From the reactions, it can be seen that the reactions (6) and (9)–(11) have higher reaction rates but the densities of the participants, O, O^+ and HO_2, are very low and the lifetimes of the participants are short. Therefore, they are not the main quenching processes. Because O_3 has a relatively long lifetime (of the order of seconds) compared with the lifetimes (of the order of microseconds or nanoseconds) of O, O^+, HO_2, etc, reaction (7) is the main quenching reaction of OH radicals.

The reason why there is no obvious change in OH intensity with increasing current is that when the applied voltage increases, the discharge voltage between the electrodes is nearly constant and the greater number of electrons emitted from the cathode result in an increase in the discharge current. More OH radicals will be produced by reactions (1)

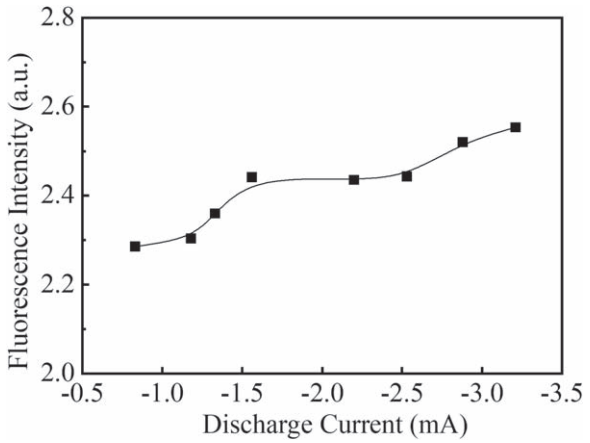

Figure 9. Fluorescence intensity of the Q1(1) branch at different discharge currents in N_2 + H_2O mixture gas.

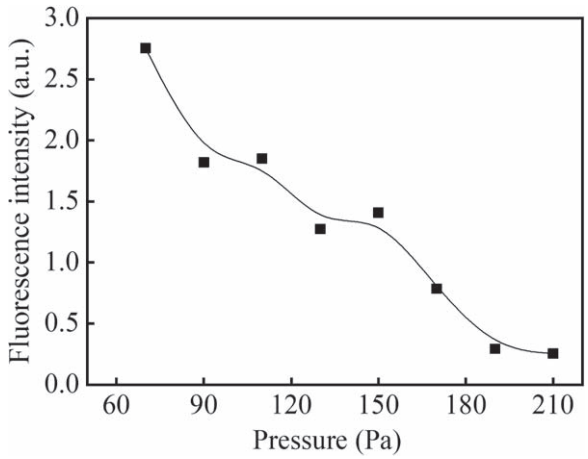

Figure 10. Fluorescence intensity of the Q1(1) branch at different pressures in N_2 + H_2O mixture gas.

and (2). But with an increase in discharge voltage, more active particles such as O_3, O, O^+ and H will be produced and quenched with OH. Therefore, the fluorescence intensity of the Q1(1) branch stays nearly constant under the investigated discharge current (applied voltage) range.

When the gas pressure in the reactor increases due to the decrease of effective electric field intensity E/N, the free path of the electrons is shortened and the density of high-energy electrons and the average energy of electrons are reduced. Although the decrease in the discharge current would induce a decrease of the voltage across the ballast resistor and an increase of the discharge voltage at a fixed applied voltage, it cannot compensate for the decrease of E/N. Therefore, the number of OH radicals generated by reactions (1) and (2) is reduced. On the other hand, when the pressure increases, the excited state OH (A) produced by the collision of the detection laser with the background gas molecules in the radiation lifetime would result in serious quenching, which will weaken the fluorescence signal of OH. Therefore, the fluorescence intensity of OH decreased significantly with an increase in pressure.

3.4. The fluorescence intensity of OH in N_2 + H_2O mixture gas

Figure 9 shows the effect of discharge current on the fluorescence intensity of the Q1(1) branch in N_2 + H_2O mixture gas with an applied voltage from −3 kV to −10 kV. The flow rate of N_2 is 40 ml min^{-1} and the pressure in the reactor is 80 Pa. From figure 9, it can be seen that the fluorescence intensity of the Q1(1) branch increases with increasing discharge current. Figure 10 shows the fluorescence intensity of the Q1(1) branch with different pressures at −4 kV applied voltage. It can be seen that the fluorescence intensity of the Q1(1) branch decreases significantly with increasing pressure within the studied pressure range from about 2.8 to 0.2.

With N_2 fills the discharge space, a large number of metastable N_2 ($A^3\Sigma_u^+$) can be generated during discharge through reaction (15) [38, 39]:

$$e + N_2 \rightarrow e + N_2(A^3\Sigma_u^+) \quad 1.1 \times 10^{-10}\ cm^3\ s^{-1}. \tag{15}$$

The metastable N_2 ($A^3\Sigma_u^+$) can produce OH radicals by colliding with water molecules [11] as shown in reaction (16):

$$N_2(A^3\Sigma_u^+) + H_2O \rightarrow OH + H + N_2 \quad 4.2 \times 10^{-11}\ cm^3\ s^{-1}. \tag{16}$$

Moreover, N_2^+ and N^+ ions can be generated by the discharge, which can react with O_3 and can effectively reduce the O_3 concentration. The reactions are as follows [40, 41]:

$$N_2^+ + O_3 \rightarrow O_2^+ + O + N_2 \quad 1 \times 10^{-10}\ cm^3\ s^{-1} \tag{17}$$

$$N^+ + O_3 \rightarrow NO^+ + O_2 \quad 5 \times 10^{-10}\ cm^3\ s^{-1}. \tag{18}$$

Due to the low excitation energy (6.02 eV) of the metastable particle N_2 ($A^3\Sigma_u^+$), the number density of energetic electrons above 6.02 eV increases significantly with increasing discharge current, and the concentration of the metastable N_2 ($A^3\Sigma_u^+$) produced by the collision of energetic electrons with N_2 is greatly increased. It can be seen from reaction (15) that a large number of OH radicals will be produced by the reaction of the particles on the metastable N_2 ($A^3\Sigma_u^+$) level of nitrogen with water molecules. The concentrations of N_2^+ and N^+ will increase correspondingly with the increase in the discharge current, and the production of O_3 will be reduced. Therefore, the fluorescence intensity of OH will be enhanced with increasing discharge current, as shown in figure 9.

When the gas pressure increases, the effective electric field intensity E/N decreases correspondingly even at a fixed applied voltage with a decreasing discharge current. The excited state OH (A) produced by the detection laser collides with other gas molecules in the radiation lifetime, resulting in serious quenching which will also weaken the fluorescence signal of OH. Therefore, increasing the pressure in the discharge reactor will lead to a significant decrease in the fluorescence intensity of OH.

3.5. The fluorescence intensity of OH in He + H_2O mixture gas

Figure 11 shows the effect of discharge current on the fluorescence intensity of the Q1(1) branch in He + H_2O mixture gas with applied voltage from −3 kV to −10 kV. The

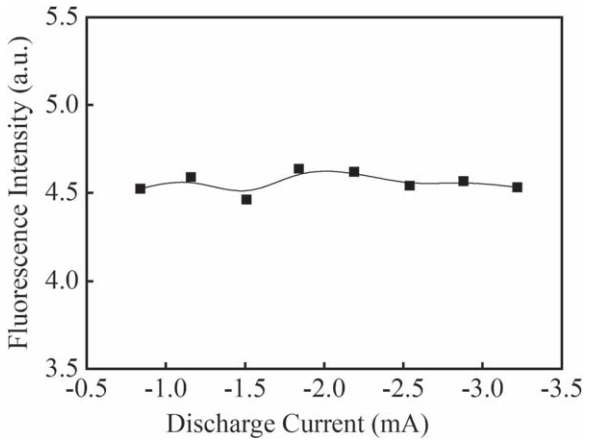

Figure 11. Fluorescence intensity of the Q1(1) branch at different discharge currents in He + H_2O mixture gas.

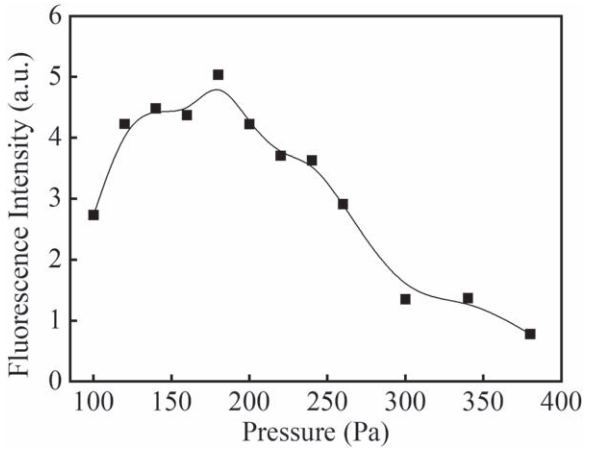

Figure 12. Fluorescence intensity of the Q1(1) branch at different pressures in He + H_2O mixture gas.

flow rate of He stays at 40 ml min^{-1} and the pressure in the reactor is 170 Pa. From figure 11, it can be seen that the fluorescence intensity of the Q1(1) branch keeps constant with increasing discharge current. When He fills the discharge space, a large number of metastable He (2^3S) particles will be generated during the discharge. The metastable He (2^3S) can generate a few active particles such as OH, O, O^+ and H by collision with H_2O molecules. The increase in the discharge current means an increase in the number of OH radicals and metastable He (2^3S) generated by direct electron collision. But more O_3, O, O^+ and H particles, which can quench OH radicals, can also be produced with a higher discharge current. Therefore, the fluorescence intensity of OH shows no obvious change with increasing discharge current within the studied range.

Figure 12 shows the variation of fluorescence intensity of the Q1(1) branch with different gas pressures at −4 kV applied voltage. It can be seen that the fluorescence intensity of the Q1(1) branch exhibits a maximum value near 180 Pa in the studied pressure range. When the gas pressure in the discharge reactor is low, the effective electric field strength E/N in the discharge space is high, the electrons can obtain more energy in the electric field and the energetic electrons can collide with molecules or atoms more effectively. However, due to the low concentration of water vapor at low pressure, the absolute number of ground state OH radicals is smaller. With an increase in gas pressure, the concentrations of water vapor and He increase, which can produce more OH radicals. Therefore, the fluorescence intensity of OH increases correspondingly. When the gas pressure exceeds 180 Pa, with the decrease of E/N and the quenching of OH radicals, the fluorescence intensity of OH decreases with increase in the gas pressure.

4. Conclusion

In this work the LIF spectra of OH ($A^2\Sigma \rightarrow X^2\Pi$ 0–0) in a needle–plate negative DC glow discharge were studied in water vapor, N_2 + H_2O mixture gas and He + H_2O mixture gas. The rotational temperature of OH ground radicals in the water vapor system was obtained by LIFBASE simulation as about 350 ± 30 K. The strongest Q1(1) rotational branch in the fluorescence spectrum of OH ($A^2\Sigma \rightarrow X^2\Pi$ 0–0) was selected to investigate the effects of the discharge current, gas pressure and different gases on the formation and quenching of OH radicals. It was found that in a pure water vapor system and He + H_2O mixture gas, the fluorescence intensity of the Q1(1) branch did not change much with increasing discharge current. With an increase in the discharge pressure from 70 Pa to 210 Pa, the fluorescence intensity of the Q1(1) branch in pure water vapor dropped by almost half from the maximum value with a decrease of E/N and quenching by the background gas molecules. In N_2 + H_2O mixture gas, the fluorescence intensity of the Q1(1) branch increased with increasing discharge current, but decreased significantly with increase in the discharge pressure from 70 Pa to 210 Pa. In the presence of metastable He molecules and a pressure increasing from 100 Pa to 380 Pa, the fluorescence intensity of the Q1(1) branch in He + H_2O mixture gas showed a maximum value at 180 Pa in the studied pressure range.

Acknowledgments

This work is supported by National Natural Science Foundation of China (No. 51777091), Innovative Talents Team Project of 'Six Talent Peaks' of Jiangsu Province (No. TD-JNHB-006), and Postgraduate Research & Practice Innovation Program of Jiangsu Province in China (No. SJCX20_0345).

References

[1] Kim K N *et al* 2016 *Thin Solid Films* **598** 315
[2] Wu S L *et al* 2020 *High Voltage* **5** 15
[3] Shan M L *et al* 2019 *Plasma Sci. Technol.* **21** 074002
[4] Tu X *et al* 2011 *J. Phys. D: Appl. Phys.* **44** 274007
[5] Laroussi M, Lu X and Keidar M 2017 *J. Appl. Phys.* **122** 020901

[6] Fridman G *et al* 2008 *Plasma Process. Polym.* **5** 503
[7] Lu X *et al* 2016 *Phys. Rep.* **630** 1
[8] Adamovich I *et al* 2017 *J. Phys. D: Appl. Phys.* **50** 323001
[9] Shao T *et al* 2018 *High Voltage* **3** 14
[10] Liu F *et al* 2008 *Spectrochim. Acta* A **69** 776
[11] Yang D Z *et al* 2012 *Plasma Sources Sci. Technol.* **21** 035004
[12] Xu N *et al* 2018 *IEEE Trans. Plasma Sci.* **46** 947
[13] Singh R, Gangal U and Gupta S K S 2012 *Plasma Chem. Plasma Process.* **32** 609
[14] Chen Y and Jin X L 2019 *Electrochim. Acta* **296** 379
[15] Wang Y X *et al* 2019 *J. Electrostat.* **98** 82
[16] Ajo P, Kornev I and Preis S 2017 *Sci. Rep.* **7** 16152
[17] Wu W W *et al* 2015 *IEEE Trans. Plasma Sci.* **43** 3979
[18] Zhang H *et al* 2016 *Plasma Chem. Plasma Process.* **36** 813
[19] Du Y J *et al* 2017 *J. Phys. D: Appl. Phys.* **50** 145201
[20] Liu F *et al* 2007 *J. Electrostat.* **65** 445
[21] Dilecce G and De Benedictis S 2011 *Plasma Phys. Controlled Fusion* **53** 124006
[22] Yue Y F *et al* 2018 *Plasma Sources Sci. Technol.* **27** 064001
[23] Liu F *et al* 2007 *Eur. Phys. J.* D **42** 435
[24] Liu F *et al* 2006 *Plasma Chem. Plasma Process.* **26** 469
[25] Yang G D *et al* 2008 *Plasma Chem. Plasma Process.* **28** 317
[26] Liu F *et al* 2017 *Plasma Sci. Technol.* **19** 064008
[27] Dilecce G *et al* 2012 *Chem. Phys.* **398** 142
[28] Sainct F P *et al* 2014 *J. Phys. D: Appl. Phys.* **47** 075204
[29] Ono R and Oda T 2008 *J. Phys. D: Appl. Phys.* **41** 035204
[30] Ono R and Tokuhiro M 2020 *Plasma Sources Sci. Technol.* **29** 035021
[31] Wu S Q *et al* 2018 *Phys. Plasmas* **25** 123507
[32] Li X C *et al* 2013 *Plasma Sci. Technol.* **15** 1149
[33] Liu F *et al* 2018 *IEEE Trans. Plasma Sci.* **46** 3194
[34] Liu F, Huang G and Ganguly B 2010 *Plasma Sources Sci. Technol.* **19** 045017
[35] Jiang C and Carter C 2014 *Plasma Sources Sci. Technol.* **23** 065006
[36] Yonemori S *et al* 2012 *J. Phys. D: Appl. Phys.* **45** 225202
[37] Ono R 2016 *J. Phys. D: Appl. Phys.* **49** 083001
[38] Kanazawa S *et al* 2020 *J. Electrostat.* **103** 103419
[39] Wang Y *et al* 2016 *IEEE Trans. Plasma Sci.* **44** 2796
[40] Ichikawa Y *et al* 2010 *Japan. J. Appl. Phys.* **49** 106101
[41] Pintassilgo C D *et al* 2010 *Plasma Sources Sci. Technol.* **19** 055001